Journal of Energy Storage 64 (2023) 107123

Contents lists available at ScienceDirect

Journal of Energy Storage

journal homepage: www.elsevier.com/locate/est

Research papers

Techno-economic assessment of wireless charging systems for airport electric shuttle buses

Zekun Guo [a], Chun Sing Lai [a,*], Patrick Luk [b], Xin Zhang [a]

[a] Department of Electronic and Electrical Engineering, Brunel University London, Uxbridge, United Kingdom
[b] Department of Engineering Systems and Management, Cranfield University, Milton Keynes, United Kingdom

ARTICLE INFO

Keywords:
Airport shuttle bus
Transportation electrification
Wireless charging technologies

ABSTRACT

Flightpath 2050, the European Commission's vision for aviation, requires that the aviation industry achieves a 75 % reduction in CO2 emissions per passenger mile and airports become emission-free by 2050. Airport shuttle buses in the airfields are going to be electrified to reduce ground emissions. Simultaneously, the airfield movement space and time schedules are becoming more limited for adopting stationary charging facilities for electrified ground vehicles. Therefore, the dynamic wireless charging technology becomes a promising technology to help improve the stability of electrification of the airfield transport network. This paper proposes a techno-economic assessment of wireless charging, wired charging, and conventional technologies for electrifying airport shuttle buses. A bi-level planning optimisation approach combines the multi-objective Non-dominated Sorting Genetic Algorithm (NSGA-III) and mixed integer linear programming (MILP) algorithm to handle a large number of decision variables and constraints generated from the investigated problem. The airport shuttle bus transport is simulated through a multi-agent-based model (MABM) approach. Four case studies are analysed for illustrating the techno-economic feasibility of wireless charging technology for airport electric shuttle buses. The results show that the wireless charging technology enables the electric shuttle buses to carry smaller batteries while conducting the same as tasks conventional diesel/petrol vehicles and the bi-directional wireless charging technology could help mitigate the impact of electrification of shuttle buses on the distribution network.

1. Introduction

As transport electrification has become an important approach to reducing emissions and mitigating pollution, the way how electric vehicles (EVs) are recharged also become a popular research topic [1,2]. However, the unavailability of charging infrastructure when EVs are away from home has become a critical challenge. Wireless power transfer technology used in EV charging might help to address the limitation of wired charging infrastructure because it does not require a physical connection between the power supply and EVs [3]. Wireless power transfer technology enables EV charging while both in stationary status and in motion by installing wireless chargers underneath the ground surface [4].

Wired EV charging systems are a mature technology with set standards [5]. These systems require a physical (ohmic) connection between EVs and the power grid through electric circuits, which consist of the ac-dc rectifier and dc-dc converters or a converter with power factor correction circuits directly from a low-frequency ac to a high-frequency ac. The wireless charging infrastructures are categorised according to the status of EVs operation while charging into the following three categories: 1) static wireless charging (SWC); 2) quasi-dynamic wireless charging (QWC); and 3) dynamic wireless charging (DWC) [3,6].

SWC means charging EVs when it is stationary [7], usually being installed in temporary public parking areas and domestic garages. SWC has a higher efficiency of power transfer than DWC because of the enhanced alignment [8]. SWC also requires a specific stationary parking area to charge the battery of the EV. However, SWC does not need any human intervention during the automatic charging procedure, which will be particularly beneficial for disabled people. The main benefit in the technological aspect of adopting SWC compared with wired EV charging technology is eliminating the shock hazards caused by wired chargers [9]. Among the three types of wireless charging technologies, SWC achieves the highest efficiency of 95 % since the alignment between EV pick-up devices and wireless charging coils is enhanced [10].

DWC technology means charging the EV when it is in motion [11,12]. It does not require the EVs to stop and wait for charging, thus

* Corresponding author.
E-mail addresses: zekun.guo@brunel.ac.uk (Z. Guo), chunsing.lai@brunel.ac.uk (C.S. Lai), p.c.k.luk@cranfield.ac.uk (P. Luk), xin.zhang@brunel.ac.uk (X. Zhang).

https://doi.org/10.1016/j.est.2023.107123
Received 22 December 2022; Received in revised form 22 February 2023; Accepted 9 March 2023
Available online 17 March 2023

the travel range of EVs would be lengthened [3]. This technology is attractive as it solves almost all problems of the EV, including range anxiety and battery cost. Similar to static wireless charging technology, the power transition between power supply units and EVs relies on the magnetic coupling effect between the transmitter coils buried underground and the EV pick-up device. A research team at the Korea Advanced Institute of Science and Technology (KAIST) lead the development of DWC technology and has installed a dynamic wireless charging system adopted to supply passenger buses [13]. An optimisation framework based on a genetic algorithm was proposed in [14] for designing the operation velocity profile of electric buses. Ref. [15] proposed a flow-capturing location model for designing the optimal location of wireless charging facilities that could maximise the demand-supply coverage. A comprehensive optimisation approach for designing dynamic wireless charging pads for EVs is presented in [16]. QWC was defined as the EV being charged when it is moving at low speed or stopped at stop-and-go positions [17]. The potential implementation positions of QWC include traffic lights, bus stops and taxi parking stands. The KAIST research group has tested a wireless charging system charging electric buses at lower power levels during its motion while charging at high power at bus stops [3], which shows the potential of quasi-dynamic charging to further improve the range of electric buses. Ref. [18] developed a novel user equilibrium model to illustrate the travel choices of electric vehicle drivers when wireless power transmitters are installed. In this work, the trade-off for vehicle speed against travel time is captured because the faster speed will make the wireless charging less efficient than the lower speed. When more and more wireless charging infrastructures are implemented, there will be more customers who choose to buy EVs and hence increase the amount of dynamic charging EVs on the traffic network [19]. The impact of different traffic scenarios (motorway, highway, and urban stretch) on wireless charging power for an ordinary EV with 24 kWh battery is compared [20], the results reveal that the EV could be recharged averagely of 0.6 kWh/km in the urban stretch and 0.25 kWh/km on the highway. Financial feasibility of DWC system has been examined in [21] for Auckland motorway, which provides essential decision support on implementation of DWC to stakeholders. Ref [22] assessed the impact of DWC implementation on the realistic driving patterns.

Similar to the vehicle-to-grid (V2G) concept of plug-in EVs, an emerging technology known as bidirectional wireless power transfer technology will potentially achieve V2G flow remotely between EVs and the power system. Ref. [23] reported the development of a large air-gap bidirectional wireless charger without an additional current chopper. Ref. [24,25] compared V2G power flow based on wired and wireless charging infrastructures. The results show that the connectivity provided by EVs with wireless connection to the grid is higher than that of wired connectivity [26], because the wireless charging infrastructure could detect the condition of EVs automatically through wireless communication devices [3]. The methodologies that enable long-term, mid-term, and short-term traffic-power network modelling and management have been reviewed in [27]. The design of a bidirectional 20 kW wireless charging system with an air gap of 11 in. is presented in [28]. A heuristic optimisation approach based on a chicken swarm algorithm for designing simply reachable charging stations for EVs is proposed in [29]. The potential of future deployment of bidirectional wireless charging facilities that will enable the EVs to charge and discharge wirelessly in regional road traffic networks is investigated in [30], which reveals that the individual entity building up the wireless charging infrastructures should be responsible for both traffic network and power network, e.g. the government agency and airport designers and operators.

The main limitation in the existing literature is the lack of techno-economic assessment of bidirectional wireless charging technology from a power system planning perspective. [31] studied the techno-economic feasibility of zero-emission microgrids with a second-life battery energy system. [32] proposed a techno-economic study of vehicle charging systems with 100 % renewable generation, hydrogen, and superconductor. The techno-economic study of energy systems with advanced technology in feasible scenarios is essential for exploring new technology solutions [33]. In this paper, the feasibility of the wireless charging system for airport electric shuttle buses is evaluated through a techno-economic assessment. One of the potential application scenarios for adopting wireless charging technology is the charging system of airport ground support vehicles. These vehicles are normally powered by gasoline and diesel engines, which would contribute to the airport's ground emissions. According to the goal set up by Flightpath 2050, the elimination of airport ground emissions is a high priority of airport operators [34], and the ambitious target towards electrifying airport ground support equipment is attracting widespread interest [35]. One of the challenges of electrifying these ground support vehicles is the limitation of space in the airfield to install charging infrastructures while the demand for ground support tasks is high [36]. Simultaneously, the airport operator has a dramatically high demand for ground support tasks, which may not permit these vehicles to stop for recharging during operation. The wireless power transfer technology will enable the power supply for airport ground support vehicles when they are moving to conduct tasks by installing wireless power transmitters underneath the airfield [37]. Ref. [38,39] proposed a novel concept of “Aviation-to-Grid (A2G)”, which describes the process of bidirectional power transfer between aviation transportation and the power grid based on wired charging. The Non-dominated Sorting Genetic Algorithm (NSGA) has been adopted for solving air traffic network improvement problems, and the results show that the algorithm performs well in the air traffic network management area [40]. In this paper, a new aviation-to-grid network nexus through adopting bidirectional Wireless power transfer technology to achieve bidirectional power transfer between airport shuttle buses and the power network is proposed.

In this paper, the bidirectional wireless charging facilities are considered to be implemented in the airfield of the commercial airport for recharging the electric shuttle buses. The proposed system will combine the airport ground-side transport network with the power grid network towards a sustainable aviation target. To evaluate the techno-economic potential of the bidirectional and unidirectional wireless charging technology, a bi-level optimisation framework is presented for seeking the optimal design of the proposed wireless charging system. There are three main contributions outlined as follows:

(1) A multi-agent-based model for airfield shuttle bus transport network simulation is proposed for generating detailed position profiles and energy consumption profiles of the shuttle buses.
(2) A bi-level optimisation framework combining the NSGA-III algorithm and mixed-integer linear programming (MILP) algorithm is proposed to solve the optimal planning problem for the wireless charging system.
(3) The techno-economic assessment of implementing airport shuttle buses powered by conventional diesel fuel, stationary wired charging, unidirectional wireless charging, and bidirectional wireless charging systems was conducted to investigate the potential cost reduction (including capital and operational costs) and support for the distribution network operation.

This paper is structured as follows: Section 2 briefly describes the key aspects of dynamic wireless charging technology for airport electric shuttle buses. The multi-agent-based model framework for airport airfield traffic network simulation is proposed in Section 3. In Section 4, the mathematical formulation of the bi-level optimisation framework that is developed from the NSGA-III algorithm and mixed integer linear programming (MILP) algorithm is presented. Case studies based on a realistic commercial airport (London City Airport) and conclusions are summarised in Sections 5 and 6, respectively.

2. Dynamic wireless charging system for airport electric shuttle buses

An increasing number of commercial airports have implemented electric vehicle fleets to eliminate airfield ground emissions, and charging infrastructures are necessary to facilitate the adoption of these electric fleets. However, the space of the airfield is valuable because of the intensity of airport movement, and the electric ground vehicle fleets could not stop tasks and turn to be recharged at stationary facilities during rush hours. Frequent plug-ins and plug-out will reduce the efficiency of airfield ground transportation. Due to the intensive flight missions and ground operation tasks, the electric ground operation vehicles on the airfields are required to be operated throughout the airport operational from 8:00 to 24:00 8:00 to 24:00 (some airports may start operations earlier depending on flight schedules), without the need for a stationary recharging. In this study, the stationary charging period for electric shuttle buses is scheduled during non-operational time (0:00 to 8:00).This means considerable battery installations on these vehicles to main the full day's demand. To address the conflicts of limited space and time schedule, and the avoidance of excessive battery weight and the associated costs, the wireless charging system becomes an appealing technology. The dynamic wireless charging system does not require the electric fleets to stop at a stationary position for recharging, the electric fleet batteries could be recharged while the fleet is in motion and conducting tasks. Importantly, battery weight could be significantly reduced.

The technology framework is shown in Fig. 1. The system is composed of wireless power transmitters (WPT) installed underneath the ground and the pick-up device installed in the electric shuttle bus. A power supply unit (PSU) is required for converting power from the distribution network to the WPT coils [41]. When the electric shuttle bus is operating on a road installed with a power transmitter, the high-frequency current in the WPTs generates a magnetic field following Ampere's Law and the magnetic field will generate a high-frequency current in the coils of the pick-up device following the Faraday's Law. Then the current is finally rectified to charge the battery of the shuttle bus. In bidirectional WPT scenario, the bus would discharge back to the grid when the battery SOC is guaranteed within the safety range (20 % to 80 % of the total energy of the battery) and there is excess power available for discharging. The bidirectional WPT enables the vehicle to both charge and discharge, depending on the requirements of the grid. The system is designed to automatically regulate the charging and discharging process, and the bus drivers would not need to be aware of this operation.

3. Multi-agent-based airport transport network simulation

The airport transport network involves complex vehicle transportation and frequent communications between different individuals. Multi-agent-based modelling (MABM) is a computational approach that enables the development of an environment where different agents are communicating and interacting with each other [42]. In this section, a multi-agent-based model is proposed to investigate the corporative behaviour of three agents involved in airport ground transportation dispatching. There are three agents in the proposed multi-agent airport transport simulation system namely, the flight agent, air traffic control agent, and shuttle bus agent. The interactions between the agents are shown in Fig. 2.

3.1. Assumptions for the simulations

This research paper determines the multi-agent-based simulations for airport transport networks based on the following assumptions:

(1) All the flight missions are considered arriving and departing punctually, the flight delays caused by weather, operation lateness, and maintenance issues are neglected.
(2) When there is no flight mission dispatched, the shuttle buses will park at the parking space close to the airport terminal buildings.
(3) Only in the cases where airports lack contact apron and jet bridge, the shuttle bus will operate to transport passengers to and from the aircraft.

The authors are aware that the proposed simulations contain a variety of uncertainties. However, this research aims to compare the wireless charging solutions for airport electric shuttle buses, rather than optimal dispatch strategy under uncertain situations. In future work, optimisation approaches designated for handling uncertainties, including stochastic optimisation, robust optimisation, chance-constrained programming-based methods, and information gap decision theory, can be adopted for optimal dispatch of the proposed airport shuttle bus wireless charging system.

3.2. Flight agent

The flight agent in this system represents the aircraft that requires boarding and deboarding services provided by airport shuttle buses. The functionality of the flight agent involves several key processes:

- The population of flight agents and their entry time into the environment are based on realistic flight demand and schedules at the airport. This means that the system takes into account real-world data and schedules to simulate the behaviour of flights and their associated services.
- When the aircraft arrives at the airport, the ground service time and departure time are determined. The flight agent then sends a service request to the air traffic control agent to notify them that shuttle bus services are required for the aircraft.

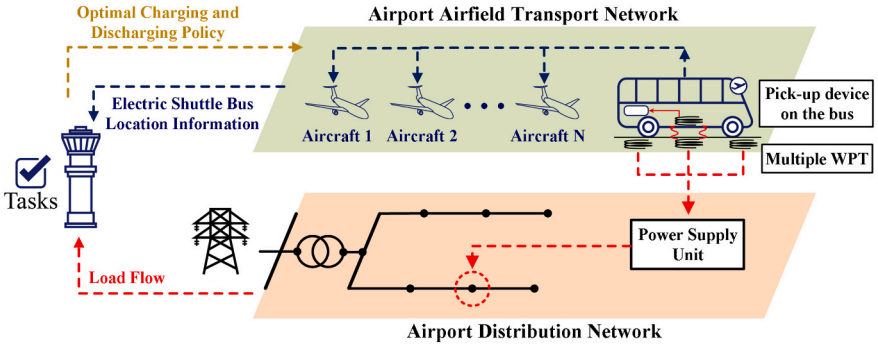

Fig. 1. Multi-agent-based dispatch framework of airport transportation network and distribution network combining by wireless charging systems for electric airport shuttle buses.

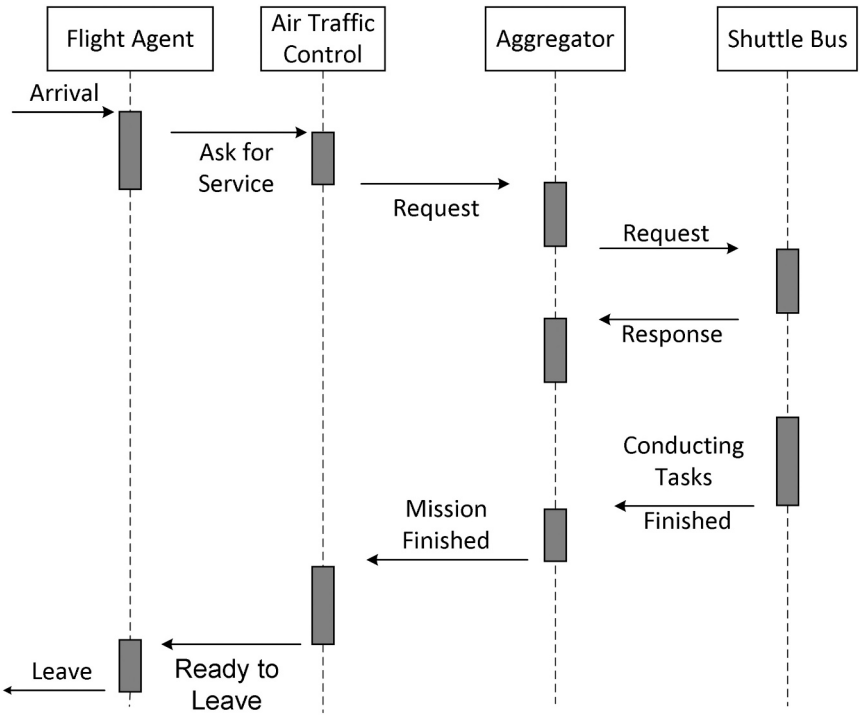

Fig. 2. The interactions between flight agent, air traffic control agent, aggregator, and shuttle bus agent.

- When the shuttle bus arrives, the passengers on the aircraft will disembark and travel to the terminal building via the shuttle buses.
- When the flight is about to depart in 15 min, the flight agent will send another request for shuttle bus services. This ensures that passengers are transported from the terminal building to the remote gates in a timely manner.

Overall, the flight agent plays a critical role in coordinating the boarding and deboarding services for aircraft at the airport. By simulating the behaviour of real-world flights and schedules, the system can accurately model and optimise the use of airport shuttle buses to ensure efficient and timely passenger transportation.

3.3. Shuttle bus agent

As mentioned in the previous section, the shuttle buses are responsible for managing the shuttle buses that transport passengers to and from the aircraft at remote gates. When the shuttle buses are not conducting a transport task, they will be part of the "Aggregator" of shuttle buses. The air traffic control agent will send task messages to the Aggregator when shuttle bus services are required to transport passengers. The shuttle bus agent records the position information and energy consumption profiles of shuttle buses. The energy consumption profiles are calculated based on the time duration of operation, which is determined by the transport tasks assigned by the air traffic control agent, as Eq. (1). Once the assigned task is completed, the shuttle bus returns to the Aggregator and becomes available for the next task. The shuttle bus agent ensures that the shuttle buses are used efficiently and effectively to transport passengers in a timely manner. The interactions between shuttle bus agents, Aggregator, and the air traffic control agent are shown in Fig. 2.

$$E_{s,t} = E_{s,t-1} - \left(1 - u_{s,t}\right) \cdot v_{s,t} \cdot f \tag{1}$$

where $E_{s,\,t}$ is the stored energy in the sth shuttle bus at time t, in kWh. $u_{s,\,t}$ is the operation status factor of shuttle buses, 1 stands for operating, and 0 stands for idling. $v_{s,\,t}$ represents the velocity of shuttle buses, in m/h. f is the energy consumption rate, in kWh/m.

3.4. Air traffic control agent

The air traffic control agent is a crucial component of the proposed MABM simulation. Its main function is to coordinate the interactions between various agents, receiving service request messages from flight agents and asking the Aggregator to assign specific shuttle buses to conduct the required services. The main processing function of the air traffic control agent is shown in Fig. 2. The air traffic control agent holds all the information about air transport movements, including the spatial information and operational status of shuttle buses and the gate and departure time of flights. It acts as a communication bridge between different agents, allowing them to share and exchange information. When the flight agents send their request messages, the air traffic control agent processes the messages and creates task requests to the Aggregator. The task requests are discrete events that allocate the appropriate vehicle agents to serve various aircraft based on the information gathered by the Aggregator. The air traffic control agent also records the position information $L_{s,\,t}$ of the shuttle buses, which is an essential profile generated by the MABM simulation.

4. Bi-level optimisation framework formulation

After the MABM simulation presented previously in Section 3, the position information and energy consumption profiles of shuttle buses are obtained. There are many requirements that need to be met for optimising the charging and discharging behaviours as well as WPT installation solutions. Most of existing studies related to the planning of energy systems with EVs solve the problems with either mixed-integer programming (MIP) or heuristic algorithms [43]. The benefits of MIP models are efficiency and accuracy through solving the problem by commercial solvers (e.g. CPLEX and Gurobi) [44]. The heuristic algorithms are capable for multi-objective optimisation problems. However, the heuristic algorithms might not be able to find optimal solutions when there is a large number of decision variables [45]. To handle a large number of constraints and decision variables, the WPT installation problem is formulated as a bi-level optimisation framework. Fig. 3 shows the overall process of the algorithm. At the primary level, the

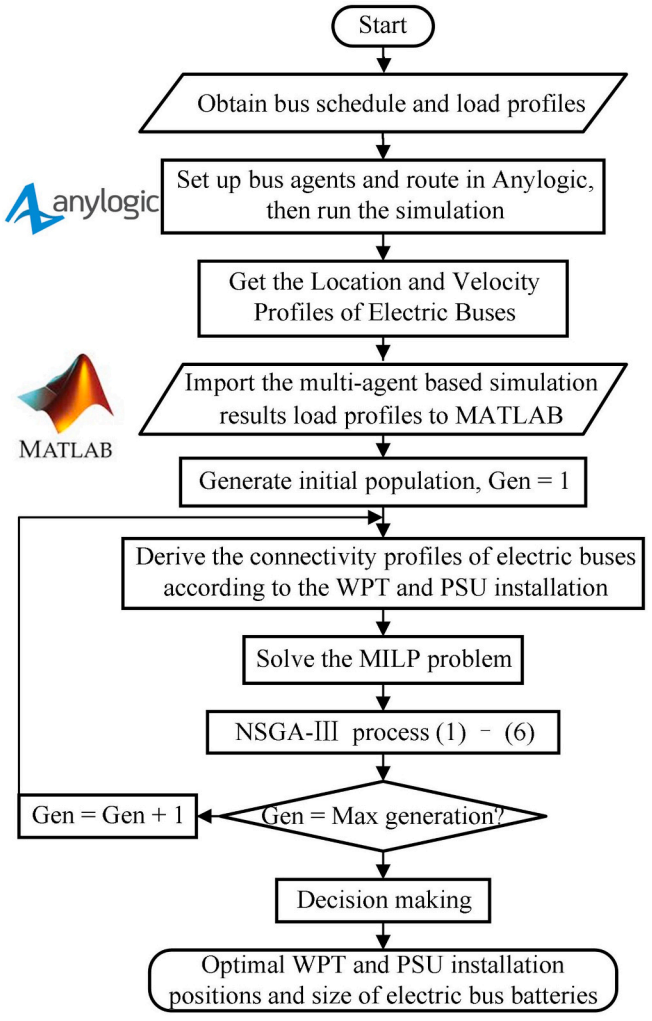

Fig. 3. Flowchart of the overall process.

Non-dominated Sorting Genetic Algorithm (NSGA-III) is adopted for deciding the WPT and PSU installation positions based on the power system voltage and power loss, which are passed to the second-level problem. The secondary level optimises the charging and discharging behaviours of the electric shuttle buses under the WPT and PSU installation decisions based on electric shuttle bus battery and charging costs and is formulated as a mixed integer linear programming (MILP) model.

4.1. NSGA-III infrastructure design

The proposed primary infrastructure design problem was solved using the effective multi-objective heuristic algorithm known as the NSGA optimisation algorithm [46], which is described in this section. Following the NSGA-II algorithm, the NSGA-III algorithm uses a reference-point-based technique presented in [47] to enhance performance while addressing multi-objective problems. The selection operator, which was created for maintaining variety among population members by updating reference points, is the only distinction between the NSGA-III algorithm and the NSGA-II algorithm. The NSGA-III optimisation technique was used to produce a number of Pareto front solutions. The reference points are selected using the Das and Denis approach [48] prior to running the NSGA-III algorithm. The trade-off between two or more objectives is displayed by the Pareto Front. The NSGA-III algorithm's logic flow is as follows:

(1) Random non-dominated sorting and crowding: Sort the particles and validate their rank to establish how far apart they are from one another as they move along fronts. The crowding distance between particles is calculated after sorting people by rank.
(2) Game selection: Binary tournament is a gaming approach for selecting two populations to participate in upcoming crossover and mutation operations. The game selection theory states that particles in a less congested zone and with a lower (better) rank are adopted first.
(3) Crossover and mutation: Following the crossover and mutation, a new population is created.
(4) Population recombination: By assessing the dominance criterion of all feasible solutions, a combined population with the parent and current populations is formed at each generation to develop non-dominant fronts.
(5) NSGA-III sorting and selection procedure: In the new generation, apply the sorting approach following three steps: (a) normalise the objective functions of the population into numbers within the range 0 to 1, (b) associate each individual of the population to a reference point, (c) perform niche preservation operation by counting the number of members of the population that are associated with reference points, and exclude the reference points that there is no member associated. Then apply the non-dominated sorting approach.
(6) New population generation: The replicated population is used to create a new generation using the same methodology as previously.

The aforementioned steps result in the generation of a set of probable optimal solutions that represent distinct energy dispatch scenarios.

$$\mathrm{P} = \{f_1(x), f_2(x), \ldots f_r(x)\}, x \in \mathbb{C} \tag{2}$$

where $\mathbb{C}$ is the feasible search space, $f_t(x)$ are sets of Pareto optimal solutions, and r is the number of populations.

The primary level makes the decisions on the installation positions of WPT and PSU, which are expressed as two sets of binary variables Θ^{wpt} and Θ^{psu}. In this work, there is no limitation on how many WPTs will be installed while only one PSU will be installed to connect all WPTs and the network.

$$\Theta^{wpt} = \{x_1, x_2, \ldots x_w\}, w \in \mathbb{R} \tag{3}$$

$$\Theta^{psu} = \{p_1, p_2, \ldots p_z\}, z \in \mathbb{N} \tag{4}$$

$$\sum_z p_z = 1 \tag{5}$$

where $\mathbb{R}$ and $\mathbb{N}$ denote collections of routes that are potentially being installed with WPT and network nodes being installed with PSU respectively.

Combining with the position information of shuttle buses $L_{s,\,t}$ obtained through MABM simulation, the connectivity information of shuttle buses could be obtained. A matrix $C_{s,\,t}$ containing full of binary parameters are created representing whether the shuttle bus is connected with the network at each time interval. For example, if the route x_w is installed with WPT, all the values in $L_{s,\,t}$ equals to x_w are set as 1 at the same position in $C_{s,\,t}$.

In each evaluation cycle, the NSGA algorithm performs power flow to avoid network constraint violations. The ac power flow is solved with the backward forward sweep (BFS) algorithm, which is an accurate and computationally efficient voltage-dependent power flow algorithm [49,50].

1) Backward sweep

The first step of the BFS algorithm is the backward sweep procedure.

In this step, the current at each bus is calculated with Kirchhoff's current law (KCL) based on the assumed value of voltage $V_{i,t}^k$. The bus current $I_{i,t}^k$ and apparent power $S_{i,t}$ are calculated as follows:

$$I_{i,t}^k = \left(\frac{S_{i,t}}{V_{i,t}^k}\right)^* \tag{6}$$

$$S_{i,t} = P_{i,t} + jQ_{i,t} = \left(P_{i,t}^G + jQ_{i,t}^G\right) - \left(P_{i,t}^L + P_{i,t}^{ES} + jQ_{i,t}^L\right) \tag{7}$$

where $P_{i,t}$ and $Q_{i,t}$ represent the real and reactive power at bus i, $P_{i,t}^G$ and $Q_{i,t}^G$ denote the real and reactive generation power output at bus i, $P_{i,t}^L$ and $Q_{i,t}^L$ are the real and reactive power consumption of conventional loads, $P_{i,t}^{ES}$ is the aggregate charging/discharging power of the WPT system.

Then the current $I_{ij,t}^k$ is calculated by summing in the backward direction from the end node j to the root node p, which is given by:

$$I_{ij,t}^k = I_{j,t}^k + \sum_p I_{jp,t}^k, p \in \Psi_j \tag{8}$$

where Ψ_j is the set of all buses that are adjacent to bus j downwards.

2) Forward sweep

The forward sweep process seeks the voltage drop from the upstream bus towards the downstream bus under the updated branch current based on Kirchhoff's Voltage Law (KVL).

$$V_{j,t}^k = V_{i,t}^k - Z_{ij} I_{ij,t}^k \tag{9}$$

where Z_{ij} is the impedance of the branch ij.

3) Voltage tolerance

The iteration convergence condition is set as the voltage difference between the current step and the previous step that has been less than the tolerance parameter σ ($\sigma = 10^{-4}$ in this work):

$$\Delta V_{j,t}^k = V_{j,t}^k - V_{j,t}^{k-1} \tag{10}$$

$$\begin{cases} \left|Re\left(\Delta V_{j,t}^k\right)\right| \le \sigma \\ \left|Im\left(\Delta V_{j,t}^k\right)\right| \le \sigma \\ \left|\Delta V_{j,t}^k\right| \le \sigma \end{cases} \tag{11}$$

When the iteration is terminated, the voltage $V_{i,t}$ and current $I_{i,t}$ at each node equal the final value of $V_{i,t}^k$ and $I_{i,t}^k$, respectively.

The apparent power of each branch $S_{br,t}$ should be within the limitation:

$$S_{br,t} = \sqrt{{P_{br,t}}^2 + {Q_{br,t}}^2} \le S_{br}^{max} \tag{12}$$

$$P_{br,t} = \sum_{ij} P_{ij,t}^G - \sum_{ij} P_{ij,t}^L \tag{13}$$

$$Q_{br,t} = \sum_{ij} Q_{ij,t}^G - \sum_{ij} Q_{ij,t}^L \tag{14}$$

The following constraints are node voltage constraints and feeder thermal limits.

$$(1-\varepsilon)V_0 \le V_{i,t} \le (1-\varepsilon)V_0 \tag{15}$$

$$I_{ij,t} \le I_{ij}^{max} \tag{16}$$

The power loss of the network P_t^{loss} can be calculated by the equation:

$$P_t^{loss} = \sum_{i,t} R_{ij}\left[\frac{\left|V_{i,t} - V_{j,t}\right|}{Z_{ij}}\right]^2 \tag{17}$$

where R_{ij} denotes the resistance of the branch ij.

The proposed primary optimisation framework has two conflict objective functions: the first objective aims to minimise the battery costs, including capital and operation and maintenance (O&M) costs for batteries, while the second objective seeks the lowest infrastructure installation costs for wireless power charging points (CAPEX) and the energy consumption cost of shuttle buses (OPEX). The power loss of the network is also included in the OPEX. Both battery costs and the CAPEX are annualised with the capital recovery factor (*CRF*), which is calculated with Eq. (21).

$$Minimise\ Obj_1 = CRF \cdot C_{batt} \cdot E_{batt} \tag{18}$$

$$Minimize\ Obj_2 = CAPEX + OPEX \tag{19}$$

$$CAPEX = CRF \cdot \sum_k \left(C_K \cdot \rho_K^C\right) \tag{20}$$

$$CRF = \frac{r \cdot (1+r)^y}{(1+r)^y - 1} \tag{21}$$

$$OPEX = 365 \cdot \left(\sum_t \left(\left(\rho_t^e + \rho_{CO_2} \cdot \vartheta^{grid}\right) \times \left(P_t^g + P_t^{loss}\right)\right) + \rho^p max\left(P_t^g\right)\right) \tag{22}$$

where the subscript K denotes the installed devices, C_K is the installed capacity of the device K, r is the discount rate, y is the number of years in the lifetime. ρ_t^e is the electricity time-of-use price, ρ_K^C is the capital cost of the device K. P_t^g is the imported grid electricity, ρ_{CO_2} is the penalty fee for CO_2 emissions. ϑ^{grid} denotes the emission factor of the grid electricity. ρ^p is the demand charges for the peak electricity demand.

The primary decision variables including installation positions of WPT and PSU will be passed to the secondary level for optimisation of charging and discharging dispatch.

4.2. Decision making

One approach for representing the best solutions in multi-objective optimisation that satisfy several goals is the Pareto optimal front. The next stage is to select between the two objectives of annualised total system cost and microgrid operating indices after acquiring the Pareto Front. There is only one possible solution from a Pareto perspective. In a variety of applications, TOPSIS has been widely employed as a multiple-attribute decision-making method based on the alternative's Euclidean distance from the positive ideal solution and the negative ideal solution [51]. The final planning option among the Pareto-optimal sites is chosen after computing the closeness degree. The two objectives are normalised by the following equation, which normalises all objectives on the same dimension scale from 0 to 1:

$$f_{nm}^{norm} = \frac{f_{nm} - min(f_{nm})}{max(f_{nm}) - min(f_{nm})} \tag{23}$$

where f_{nm} is the value of nth solution of mth objective.

The "ideal" and "nadir" points, which stand for the best and worst positions, respectively, are used as two reference points by the TOPSIS technique to choose the optimum compromising solution. The smallest Euclidean distances between "ideal" and "nadir" locations and non-dominated solutions are ED_{n+} and ED_{n-}, respectively.

$$ED_{n+/n-} = \sqrt{\sum_{m=1}^{N_{obj}} \left(f_{nm} - f_{nm}^{ideal/nadir}\right)} \tag{24}$$

The lower the value of ED_{n+}, the closer the solution is to the optimum

decision point. The relative closeness index is calculated using Euclidean distance, as presented in (25). The overall ideal solution is determined by the solution with the highest relative closeness index.

$$\pi_n = \frac{ED_{n-}}{ED_{n+} + ED_{n-}} \tag{25}$$

The solutions are ranked in ascending order according to the value of π_n, and the solution with the maximum relative closeness index (π_n) is then selected as the final ideal solution of the optimisation problem.

4.3. MILP-based wireless charging management

The secondary layer problem was formulated with mixed integer linear programming (MILP) because the problem contains many decision variables and constraints in the heuristic algorithm that could not manage, but MILP formulation will be more efficient for solving this type of problem. The MILP problem is solved for each evaluation of the population generated in the NSGA-III algorithm. The MILP problem aims to derive the optimal charging/discharging dispatch profile of electric shuttle buses under the current WPT and PSU installation choice of the individual in the NSGA-III algorithm.

The charging constraints are translated from the transportation profiles of electric shuttle buses, including the energy consumption profile $E^{cons}_{s,t}$ and the connectivity profile $C_{s,t}$. The charging and discharging behaviour are controlled by two binary variables $u^{ch}_{s,t}$ and $u^{disc}_{s,t}$, respectively.

$$u^{ch}_{s,t} + u^{disc}_{r,t} \leq 1 \tag{26}$$

$$P^{ch}_{s,t} = u^{ch}_{s,t} \cdot P^{rated} \tag{27}$$

$$P^{disc}_{s,t} = u^{disc}_{s,t} \cdot P^{rated} \tag{28}$$

The connectivity of electric shuttle buses and WPTs are expressed as a matrix $C_{s,t}$, if the sth electric shuttle bus is connected to one installed WPT at time t, the value of the $C_{s,t}$ equals one, otherwise, the value is zero.

The power limit for the connectivity of electric shuttle buses and WPTs is shown in the following equation:

$$P^{disc}_{s,t}, P^{ch}_{s,t} \leq C_{s,t} \cdot P^{rated} \tag{29}$$

The stored energy of each shuttle bus is expressed as follows:

$$E^{batt}_{s,t} = E^{batt}_{s,t-1} + \eta^{ch} \cdot P^{ch}_{s,t} - \eta^{disc} \cdot P^{disc}_{s,t} - E^{cons}_{s,t-1} \tag{30}$$

$$E^{batt}_{s,0} = E^{batt}_{s,T} \tag{31}$$

$$0.2 \cdot E^{max} \leq E^{batt}_{s,t} \leq E^{max} \tag{32}$$

The aggregate charging/discharging power of shuttle buses is formulated as follows:

$$P^{ES}_{t} = \sum_{s} \left(P^{ch}_{s,t} - P^{disc}_{s,t} \right) \tag{33}$$

After solving the MILP problem, the total charging power of electric shuttle buses is passed back to the NSGA-III algorithm for power flow compliance analysis.

4.4. Secondary objective function

The secondary level problem aims to minimise the annualised cost of the electric shuttle bus batteries as well as the annual electricity purchase cost of charging power.

$$Minimise \left(CRF \cdot C^{batt} \cdot N_{ev} \cdot E^{max} + 365 \cdot \sum_{i} \sum_{t} \rho^{e}_{t} \cdot P^{ES}_{t} \right) \tag{34}$$

5. Case studies

To show how to apply the proposed approach to real-world scenarios, a detailed case study investigated the London City Airport (IATA code: LCY), which is a regional airport with a standard linear terminal building that lies in London, England. The airfield transport network and power network topologies of LCY airport are shown in Fig. 5, with the location of the power network nodes (N1–N9), gate position numbers (G1 – G24), and shuttle bus transport route numbers (R1 – R18). It is worth noting that in our study, the power network supplying LCY airport is assumed to be IEEE 9-bus radial distribution network, and each node is located at one contact gate at the terminal building. The candidate installation positions of WPT and PSU are all power network nodes and shuttle bus transport routes. The wired charging facilities cannot be installed in the routes of aircraft and ground support equipment and must be installed close to buildings for safety reasons. Based on our assessment, the selected area was found to be the best option due to its proximity to the shuttle bus route, electrical network constraints, and minimum disruption to airport operations. As a result, the electric shuttle buses are assumed to recharge wired stationarily at the station area. The flight demand on one of the busiest days (31st March) at LCY airport in 2019 is selected in this simulation, as shown in Fig. 4. The total number of shuttle buses has been set at 60, which is the minimum required to support the operation of LCY Airport during peak demand days without causing delays, based on our simulation tests. The energy consumption rate of the shuttle bus is 0.32 L/km for diesel and 1.27 kWh/km for electricity, which are taken from [52]. The speed of shuttle buses is set as 15 miles per hour. The line and load data of the IEEE 9-bus radial distribution network is shown in Table 1. The economic parameters and energy factors are shown in Tables 2 and 3, respectively.

There are two benchmark scenarios: Case 1: no electrification, all shuttle buses are using diesel; Case 2: wired charging; and two investigated scenarios: Case 3: wireless charging; Case 4: bidirectional wireless charging.

1) Case 1: Electrification is not considered; the shuttle buses will remain using conventional diesel fuel.
2) Case 2: The electric shuttle buses are assumed to recharge stationarily at the station area charging facilities, which are connected to node 9 of the distribution network, as shown in Fig. 5. This case assumes that all electric buses are equipped with batteries that are fully charged at the beginning of the day and that can meet the power requirements of the day's flight service missions. In this case, a regular AC charger with a rated power of 50 kW is used to charge the buses during the off-peak period from 0:00 to 6:00 when the airport is not in operation. The required energy capacity of the electric shuttle bus battery is 174.5 kWh while the total required number of chargers is 33.

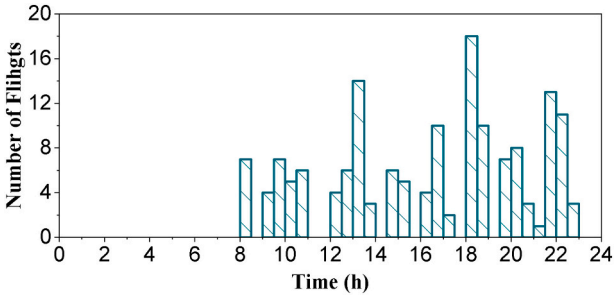

Fig. 4. Flight demand at LCY airport on 31st March 2019 on a half-hourly basis.

Table 1
Line and load data of the IEEE 9 bus radial test system.

	Bus number								
	1	2	3	4	5	6	7	8	9
P (kW)	1840	980	1790	1598	1610	780	1150	980	1640
Q (kVar)	460	340	446	1840	600	110	60	130	200
i bus	0	1	2	3	4	5	6	7	8
j bus	1	2	3	4	5	6	7	8	9
$R_{i,j}$ (Ω)	0.1233	0.0140	0.7463	0.6984	1.9831	0.9053	2.0552	4.7953	5.3434
$X_{i,j}$ (Ω)	0.4127	0.6051	1.2050	0.6084	1.7276	0.7886	1.1640	2.7160	3.0264

Table 2
Economic parameters of technologies [37].

Device	Installation cost	Maintenance cost	Cases
WPT	89,264 £/mile	892 £/mile per year	3, 4
PSU	10,000 £/each	100 £/year	3, 4
Pickup device	5000 £/each	–	3, 4
EV 50 kW Chargers	2500 £/each	250 £/10 years	2

Table 3
Energy prices/factors of airport power system.

Parameter	Value	Ref
Fuel price	1.3 £/kg	[53]
CO_2 Emission factor of diesel fuel	2.68 kg/L	[54]
CO_2 Emission factor of electricity	0.257 kg/kWh	[55]
CO_2 Emission cost	75 £/t	[56]

3) Case 3: The electric shuttle buses will be able to charge wirelessly through installed unidirectional WPT and PSU. It is assumed that the PSU connects with multiple WPTs through the closest WPT.
4) Case 4: The electric shuttle buses will be able to interact with the distribution network by charging or discharging power through bidirectional WPT and PSU.

The MABM simulation is implemented in the Anylogic software, and the bi-level optimisation framework is developed in the MATLAB 2021a environment and solved with the Gurobi solver and YALMIP software. All the modelling and simulations are conducted on a PC with AMD Ryzen 5 3500 @ 3.6 GHz processor and 16 GB RAM. The multi-agent-based simulation takes 1 min 12 s while the optimisation times for Case 3 and Case 4 are 25 min and 41.5 min respectively. The time of use (TOU) pricing mechanism of electricity price is introduced as £0.07 (00:00–07:00), £0.15 (10:30–16:00 and 21:00–24:00), and £0.2 (07:00–10:30 and 16:00–21:00) per kWh, with an additional demand charge of £0.2 per kW per day. The demand charge will be calculated based on the maximum power demand during the operation.

5.1. Pareto fronts

The resulting non-dominated Pareto front solutions of Case 3 and Case 4 are shown in Fig. 6. The annualised CPEX and OPEX for the Pareto solutions in Case 3 are between 0.36 and 0.39 million pounds, while the figure in Case 4 varies from 0.40 to 0.45 million pounds. This significant increase in the CAPEX and OPEX is mainly due to the consequence of the energy injected by electric shuttle buses through bidirectional wireless charging transmitters. As seen in Fig. 6, the optimal population of Case 4 seems to have higher values of the battery cost, this is because the bidirectional wireless charging option might make them decide to carry larger batteries to inject power back into the grid for reducing the grid electricity cost and network power loss cost.

The optimal WPT installation positions for Case 3 and Case 4 are shown in Fig. 7(a) and (b), respectively. The distance from PSU to the closest WPT is around 68 m. There are 7 routes installed with WPT in both cases, while the PSU is installed on node 4 in Case 3 and on node 8 in Case 4. This is because the shuttle buses with sole-directional wireless charging are loads, but the shuttle buses with bi-directional wireless charging work as energy storage units. The former tends to be installed on the upstream node while the latter tends to be installed on the downstream node. These are reasonable choices for operating in radial distribution networks in terms of reducing power loss and reducing voltage drop. The aggregation of bidirectional wireless charging shuttle buses works as a large energy storage unit in the airport distribution network.

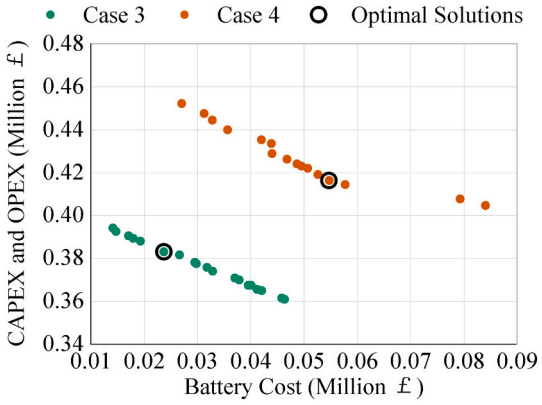

Fig. 6. Pareto fronts of Case 3 and Case 4.

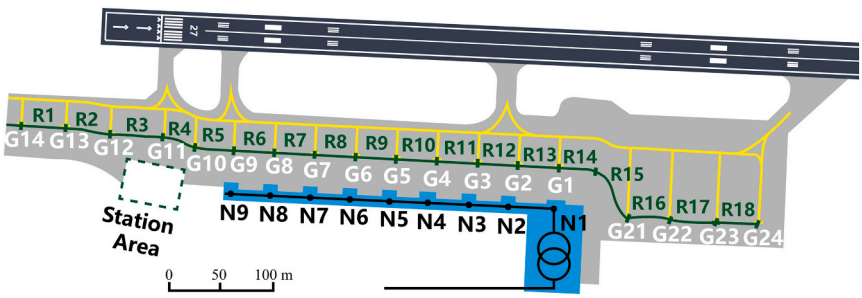

Fig. 5. The airport ground transportation network and the IEEE 9-bus radial distribution network framework at London City Airport (LCY).

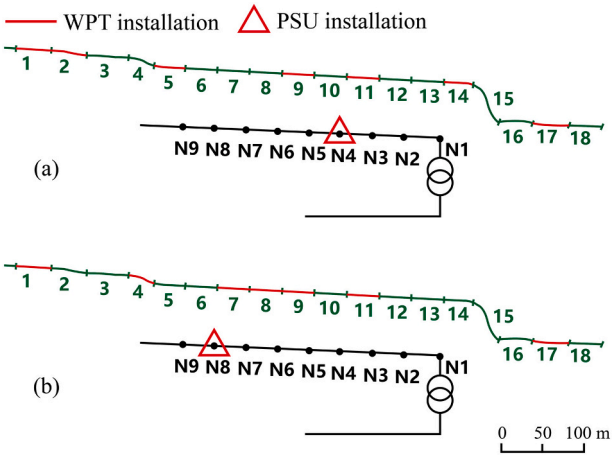

Fig. 7. WPT and PSU installation positions. (a) Case 3: wireless charging, (b) Case 4: bidirectional wireless charging.

5.2. Charging power and aggregate stored energy

Figs. 8 and 9 show the electric shuttle bus charging power dispatch and the aggregate stored energy in the shuttle bus fleet. As shown in Fig. 9(a), the electric shuttle buses recharge during the early morning (1 to 5 am) when there is no flight demand because the fleet is in use during the daytime. As a result, the electric buses have to carry large size batteries to guarantee the daytime energy consumption is met, as shown in Fig. 8. By contrast, the wireless charging demand of electric buses is mainly distributed evenly during the daytime, as shown in Fig. 9(b) and (c). The bidirectional wireless charging power discharges during the morning peak (8–10 am) of the electricity demand of the terminal building. Table 4 compared the characteristics of the demand profile of Cases 2, 3, and 4. The results show that the Case 3, which used wireless charging technology, had similar peak and average demand values as Case 2, which used wired charging technology. This suggests that wireless charging can provide the same level of power output and charging capacity as wired charging, while eliminating the need for physical connections between the vehicle and the charger. The results also show that Case 4, which used bidirectional wireless charging technology, had a higher peak demand value than Cases 2 and 3, but a similar average demand value. This is because bidirectional wireless charging allows energy to be transferred between the vehicle and the grid, enabling the vehicle to serve as a mobile energy storage system. This feature can help to balance the power grid and provide additional flexibility and resilience in managing the electric power system.

5.3. Voltage deviation

The bus voltage profiles and voltage variation profiles across time for four cases are illustrated in Fig. 10(a) and (b), respectively. As the

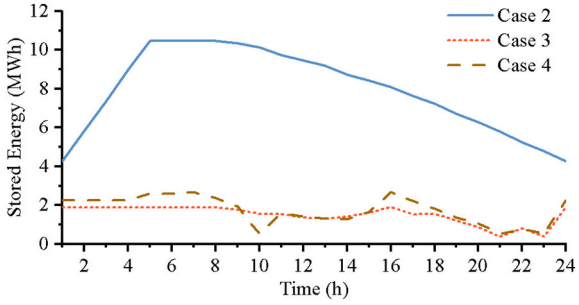

Fig. 8. Aggregate energy storage of all-electric shuttle buses in Case 2, Case 3 and Case 4.

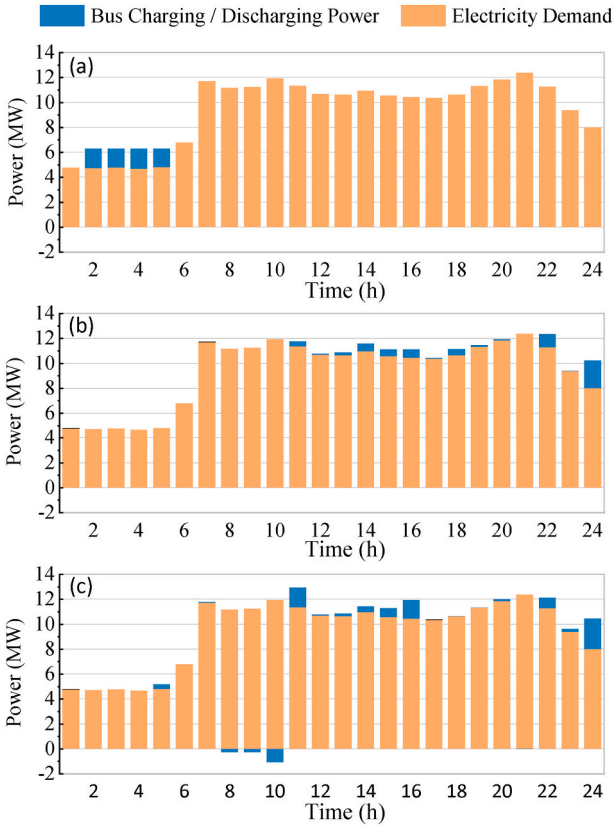

Fig. 9. Airport electricity demand and the charging and discharging power of electric shuttle buses dispatch results for (a) Case 2, (b) Case 3, and (c) Case 4.

Table 4
Comparison of demand characteristics between three cases.

Cases	Peak demand (MW)	Average demand (MW)	Peak hour	Annual electricity charges	
				TOU charge (million £)	Demand charge (million £)
2	12.37	9.69	21:00	6.37	0.12
3	12.37	9.72	21:00	6.47	0.11
4	12.94	9.73	11:00	6.43	0.18

reference case, the voltage profile of Case 1 is the highest among the four cases and varies with the basic electric load curve through 24 h. It can be seen from Fig. 10(a) that the voltage of Case 2 drops from 0.98 to 0.96 during the night-time hours (1 to 5 am) because of the highly intensive power drawn by the stationary charging shuttle buses. It also seems that the voltage at node 9 drops sharply by 1 %, which is most remarkable among the four cases, as shown in Fig. 10(b). It appears that the voltage profile of Case 3 fluctuates more during the daytime and drops most significantly at 14:00 and 24:00 by 0.16 % and 0.77 % respectively. The voltage profile in Case 4 is almost overlapped with Case 1, showing that the bi-directional wireless charging scenario has the lowest impact on the network operation in terms of voltage deviation compared with other shuttle bus electrification scenarios. Overall, the voltage deviations caused by the proposed cases are not too severe. However, the results also imply that the adoption of wireless charging or wired charging might pose a potential threat to the operation of airport distribution networks. Apparently, the flexibility of bidirectional wireless charging could help mitigate the impact of airport ground vehicle electrification.

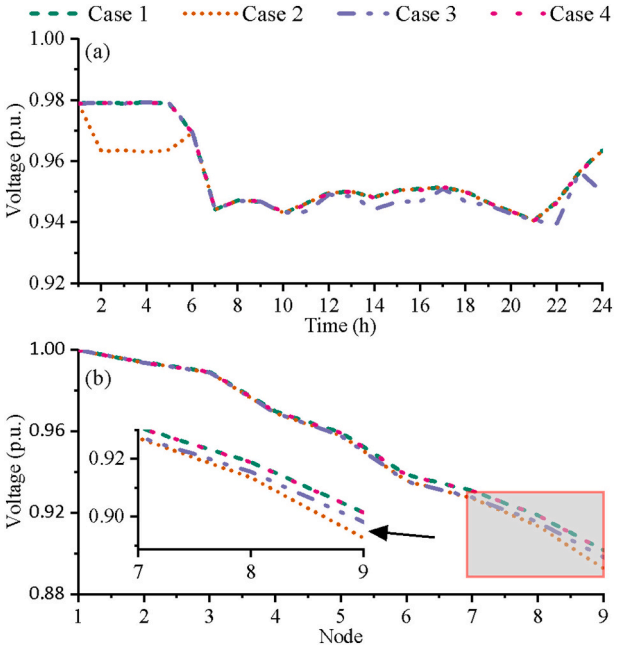

Fig. 10. Average voltage profiles for all four cases

5.4. Economic analysis

The total annualised cost results for the four cases are presented in Fig. 11. The annualised costs of conventional diesel shuttle buses (Case 1) are significantly higher than electrification cases (Case 2 - 4), mainly caused by the fuel price. Among the electrification cases, the plug-in charging option has a higher cost from the larger size of batteries, while the electricity cost will be less because of the lower electricity price during night-time. The cost of bidirectional wireless charging technology (Case 4) is generally higher than that of unidirectional wireless charging (Case 3), but it is still lower than the cost of traditional wired charging systems which require significant large battery capacity. There is a trend that the electric shuttle buses would prefer to carry a larger battery when there is a bidirectional charging option available, which is consistent with the analysis in previous sections. While the higher cost of bidirectional wireless charging systems may be a limiting factor in some cases, the potential benefits of enhanced grid resilience and flexibility may outweigh these costs in certain contexts.

It is worth noting that, the emission cost of Case 1 is 159 %, 132 % and 120 % higher than that of Case 2, Case 3 and Case 4, respectively. This shows that the emission tax might be a vital factor that will push airport designers and operators to consider the electrification of shuttle fleets as soon as possible to avoid high carbon tax in the future.

6. Conclusion

This paper proposes a techno-economic assessment of wireless charging, wired charging, and conventional technologies for electrifying airport shuttle buses. A bi-level optimisation approach for allocating WPTs and PSU in the airfield traffic network and distribution power network of a commercial airport is proposed. Four case studies are analysed for illustrating the techno-economic feasibility of wireless charging technology for airport electric shuttle buses. The bi-directional wireless charging technology could help mitigate the impact of the electrification of shuttle buses on the distribution network because there are fewer voltage drops during the operation time. The economic analysis shows that the annualised operation cost of conventional diesel shuttle buses is far more expensive in the future, which makes electrification a promising option. The wireless charging technology enables

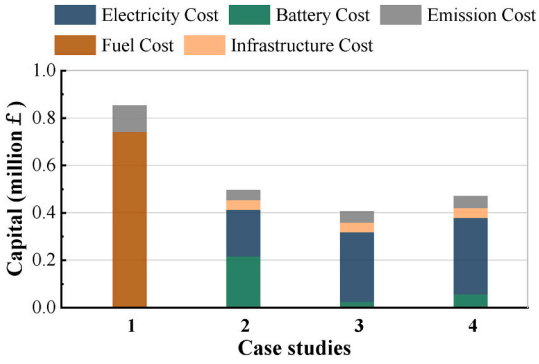

Fig. 11. Annualised costs of all four cases.

the electric shuttle buses to carry smaller batteries while conducting the same tasks. The bi-directional wireless charging shuttle buses might carry larger batteries for reducing the overall cost by injecting power back into the grid and reducing power loss. In summary, future airport designers and operators are highly likely to electrify the ground vehicles in the airside of the airport, and wireless charging technology could be an attractive option for both technological (in terms of distribution network operation) and economic reasons. A real-life example has been used to demonstrate the benefits gained with the present approach. Future research will explore the potential of the cooperation between electric ground support vehicles and airport parking lot EVs and future adopted electric aircraft. And the feasibility of wireless charging technology on road traffic and ordinary electric vehicles could be investigated as well.

CRediT authorship contribution statement

Zekun Guo: Conceptualization, Methodology, Software, Data curation, Writing - Original draft preparation, Writing - Reviewing and Editing. **Chun Sing Lai**: Conceptualization, Methodology, Writing - Original draft preparation, Writing - Reviewing and Editing, Supervision, Funding acquisition, Project Administration. **Patrick Luk**: Conceptualization, Methodology, Writing - Original draft preparation. **Xin Zhang**: Conceptualization, Writing - Reviewing and Editing, Supervision.

Data Access Statements

Data supporting this study are included within the article.

Declaration of competing interest

The authors declare that they have no known competing financial interests or personal relationships that could have appeared to influence the work reported in this paper.

Data availability

Data will be made available on request.

Acknowledgements

We are grateful for support from the DTE Network+ funded by EPSRC grant reference EP/S032053/1.

References

[1] H.S. Das, M.M. Rahman, S. Li, C.W. Tan, Electric vehicles standards, charging infrastructure, and impact on grid integration: a technological review, Renew. Sust. Energ. Rev. 120 (2020), https://doi.org/10.1016/j.rser.2019.109618.

[2] S. Hemavathi, A. Shinisha, A study on trends and developments in electric vehicle charging technologies, J. Energy Storage 52 (2022), 105013, https://doi.org/10.1016/j.est.2022.105013.

[3] A. Ahmad, M.S. Alam, R. Chabaan, A comprehensive review of wireless charging technologies for electric vehicles, IEEE Trans. Transport. Electrif. 4 (2017) 38–63, https://doi.org/10.1109/TTE.2017.2771619.

[4] J. Sun, T. Jiang, G. Yang, Y. Tang, S. Chen, S. Qiu, K. Song, A novel charging and active balancing system based on wireless power transfer for Lithium-ion battery pack, J. Energy Storage 55 (2022), 105741, https://doi.org/10.1016/j.est.2022.105741.

[5] H.S. Das, M.M. Rahman, S. Li, C.W. Tan, Electric vehicles standards, charging infrastructure, and impact on grid integration: a technological review, Renew. Sust. Energ. Rev. (2019), https://doi.org/10.1016/j.rser.2019.109618.

[6] Y.J. Jang, Survey of the operation and system study on wireless charging electric vehicle systems, Transp Res Part C Emerg Technol. 95 (2018) 844–866, https://doi.org/10.1016/j.trc.2018.04.006.

[7] S. Lukic, Z. Pantic, Cutting the cord: static and dynamic inductive wireless charging of electric vehicles, IEEE Electrif. Mag. 1 (2013) 57–64, https://doi.org/10.1109/MELE.2013.2273228.

[8] A. Mahesh, B. Chokkalingam, L. Mihet-Popa, Inductive wireless power transfer charging for electric vehicles-a review, IEEE Access. 9 (2021) 137667–137713, https://doi.org/10.1109/ACCESS.2021.3116678.

[9] X. Lu, P. Wang, D. Niyato, D.I. Kim, Z. Han, Wireless charging technologies: fundamentals, standards, and network applications, IEEE Communications Surveys and Tutorials 18 (2016) 1413–1452, https://doi.org/10.1109/COMST.2015.2499783.

[10] K. van Schuylenbergh, R. Puers (Eds.), Primary coil drivers, in: Inductive Powering: Basic Theory and Application to Biomedical Systems, Springer, Netherlands, Dordrecht, 2009, pp. 103–143, https://doi.org/10.1007/978-90-481-2412-1_4.

[11] LA, J. Jiang, A. Maglaras, FV, S. Moschoyiannis, Dynamic wireless charging of electric vehicles on the move with mobile energy disseminators, International Journal of Advanced Computer Science and Applications 6 (2015) 239–251, https://doi.org/10.14569/ijacsa.2015.060634.

[12] P.K. Joseph, D. Elangovan, A review on renewable energy powered wireless power transmission techniques for light electric vehicle charging applications, J. Energy Storage 16 (2018) 145–155, https://doi.org/10.1016/j.est.2017.12.019.

[13] Y.D. Ko, Y.J. Jang, The optimal system design of the online electric vehicle utilizing wireless power transmission technology, IEEE Trans. Intell. Transp. Syst. 14 (2013) 1255–1265, https://doi.org/10.1109/TITS.2013.2259159.

[14] Y.D. Ko, Y.J. Jang, Efficient design of an operation profile for wireless charging electric tram systems, Comput. Ind. Eng. 127 (2019) 1193–1202, https://doi.org/10.1016/j.cie.2018.03.042.

[15] R. Riemann, D.Z.W. Wang, F. Busch, Optimal location of wireless charging facilities for electric vehicles: flow capturing location model with stochastic user equilibrium, Transp Res Part C Emerg Technol. 58 (2015) 1–12, https://doi.org/10.1016/j.trc.2015.06.022.

[16] R. Tavakoli, E.M. Dede, C. Chou, Z. Pantic, Cost-efficiency optimization of ground assemblies for dynamic wireless charging of electric vehicles, IEEE Trans, Transport. Electrif. 8 (2022) 734–751, https://doi.org/10.1109/TTE.2021.3105573.

[17] Y.J. Jang, S. Jeong, M.S. Lee, Initial energy logistics cost analysis for stationary, quasi-dynamic, & dynamicwireless charging public transportation systems, Energies (Basel). 9 (2016), https://doi.org/10.3390/en9070483.

[18] Z. Chen, F. He, Y. Yin, Optimal deployment of charging lanes for electric vehicles in transportation networks, Transp. Res. B Methodol. 91 (2016) 344–365, https://doi.org/10.1016/j.trb.2016.05.018.

[19] H. Liu, D.Z.W. Wang, Locating multiple types of charging facilities for battery electric vehicles, Transp. Res. B Methodol. 103 (2017) 30–55, https://doi.org/10.1016/j.trb.2017.01.005.

[20] C.A. García-Vázquez, F. Llorens-Iborra, L.M. Fernández-Ramírez, H. Sánchez-Sainz, F. Jurado, Comparative study of dynamic wireless charging of electric vehicles in motorway, highway and urban stretches, Energy 137 (2017) 42–57, https://doi.org/10.1016/j.energy.2017.07.016.

[21] R.C. Majhi, P. Ranjitkar, M. Sheng, Assessment of dynamic wireless charging based electric road system: a case study of Auckland motorway, Sustain. Cities Soc. 84 (2022), 104039, https://doi.org/10.1016/j.scs.2022.104039.

[22] G. Duarte, A. Silva, P. Baptista, Assessment of wireless charging impacts based on real-world driving patterns: case study in Lisbon, Portugal, Sustain. Cities Soc. 71 (2021), https://doi.org/10.1016/j.scs.2021.102952.

[23] J.Y. Lee, B.M. Han, A bidirectional wireless power transfer EV charger using self-resonant PWM, IEEE Trans. Power Electron. 30 (2015) 1784–1787, https://doi.org/10.1109/TPEL.2014.2346255.

[24] Y. Tang, Y. Chen, U.K. Madawala, D.J. Thrimawithana, H. Ma, A new controller for bidirectional wireless power transfer systems, IEEE Trans. Power Electron. 33 (2018) 9076–9087, https://doi.org/10.1109/TPEL.2017.2785365.

[25] C. Xia, W. Wang, Y. Liu, K. Lin, Y. Wang, X. Wu, A bidirectional wireless power transfer system for an electric vehicle with a relay circuit, Turk. J. Electr. Eng. Comput. Sci. 25 (2017) 3037–3051, https://doi.org/10.3906/elk-1609-75.

[26] X. Huang, H. Qiang, Z. Huang, Y. Sun, J. Li, The interaction research of smart grid and EV based wireless charging, 2013 9th IEEE vehicle power and propulsion conference, IEEE VPPC 2013 (2013) 354–358, https://doi.org/10.1109/VPPC.2013.6671718.

[27] Y. Sun, P. Zhao, L. Wang, S.M. Malik, Spatial and temporal modelling of coupled power and transportation systems: a comprehensive review, Energy Conversion and Economics. 2 (2021) 55–66, https://doi.org/10.1049/enc2.12034.

[28] M. Mohammad, O.C. Onar, G.-J. Su, J. Pries, V.P. Galigekere, S. Anwar, E. Asa, J. Wilkins, R. Wiles, C.P. White, L.E. Seiber, Bidirectional LCC–LCC-compensated 20-kW wireless power transfer system for medium-duty vehicle charging, IEEE Transactions on Transportation Electrification. 7 (2021) 1205–1218, https://doi.org/10.1109/TTE.2021.3049138.

[29] S. Sachan, S. Deb, S.N. Singh, P.P. Singh, D.D. Sharma, Planning and operation of EV charging stations by chicken swarm optimization driven heuristics, Energy Convers. Econo. 2 (2021) 91–99, https://doi.org/10.1049/enc2.12030.

[30] H. Nasr Esfahani, Z. Liu, Z. Song, Optimal pricing for bidirectional wireless charging lanes in coupled transportation and power networks, Transp Res Part C Emerg Technol. 135 (2022), 103419, https://doi.org/10.1016/j.trc.2021.103419.

[31] A. Bhatt, W. Ongsakul, N.M. Madhu, Optimal techno-economic feasibility study of net-zero carbon emission microgrid integrating second-life battery energy storage system, Energy Convers Manag. 266 (2022) 115825, https://doi.org/10.1016/j.enconman.2022.115825.

[32] X. Chen, Z. Pang, M. Zhang, S. Jiang, J. Feng, B. Shen, Techno-economic study of a 100-MW-class multi-energy vehicle charging/refueling station: using 100 % renewable, liquid hydrogen, and superconductor technologies, Energy Convers. Manag. 276 (2023), 116463, https://doi.org/10.1016/j.enconman.2022.116463.

[33] X. Zhang, P. Elia Campana, X. Bi, M. Egusquiza, B. Xu, C. Wang, H. Guo, D. Chen, E. Egusquiza, Capacity configuration of a hydro-wind-solar-storage bundling system with transmission constraints of the receiving-end power grid and its techno-economic evaluation, Energy Convers. Manag. 270 (2022), https://doi.org/10.1016/j.enconman.2022.116177.

[34] Flightpath 2050, Europe's Vision for Aviation; Maintaining Global Leadership and Serving Society's Needs: Report of the High-Level Group on Aviation Research, Publications Office of the European Union, Luxembourg, 2012, https://doi.org/10.2777/50266.

[35] M. Lukic, P. Giangrande, A. Hebala, S. Nuzzo, M. Galea, Review, Challenges, and future developments of electric taxiing systems, IEEE Trans. Transport. Electrif. 5 (2019) 1441–1457, https://doi.org/10.1109/TTE.2019.2956862.

[36] S. Helber, J. Broihan, Y.J. Jang, P. Hecker, T. Feuerle, Location planning for dynamicwireless charging systems for electric airport passenger buses, Energies (Basel) 11 (2018) 1–16, https://doi.org/10.3390/en11020258.

[37] L. Soares, H. Wang, Economic feasibility analysis of charging infrastructure for electric ground fleet in airports, Transp. Res. Rec. 2675 (2021) 1–12, https://doi.org/10.1177/03611981211033859.

[38] Z. Guo, X. Zhang, N. Balta-Ozkan, P. Luk, Aviation to grid: airport charging infrastructure for electric aircraft, in: Proceedings of 12th International Conference on Applied Energy, Part 2 10, 2021. Thailand/Virtual.

[39] Z. Guo, J. Zhang, R. Zhang, X. Zhang, Aviation-to-grid flexibility through electric aircraft charging, IEEE Trans. Ind. Inform. 1 (2021), https://doi.org/10.1109/TII.2021.3128252.

[40] Q. Cai, S. Alam, V. Duong, On robustness paradox in air traffic networks, IEEE Trans. Netw. Sci. Eng. 7 (2020) 3087–3099, https://doi.org/10.1109/TNSE.2020.3015728.

[41] L. Guo, H. Wang, A novel design of partially magnetized pavement for wireless power transfer to electric vehicles with improved efficiency and cost saving, Energy Convers. Manag. 252 (2022), 115080, https://doi.org/10.1016/j.enconman.2021.115080.

[42] O. Bucovetchi, A. Georgescu, D. Badea, R.D. Stanciu, Agent-based modeling (ABM): support for emphasizing the air transport infrastructure dependence of space systems, Sustainability (Switzerland). 11 (2019), https://doi.org/10.3390/su11195331.

[43] S.M. Bagher Sadati, J. Moshtagh, M. Shafie-khah, A. Rastgou, J.P.S. Catalão, Operational scheduling of a smart distribution system considering electric vehicles parking lot: a bi-level approach, International Journal of Electrical Power and Energy Systems. 105 (2019) 159–178, https://doi.org/10.1016/j.ijepes.2018.08.021.

[44] J. Mo, X. Dai, S. Xu, L. Shi, Design method of combined cooling, heating, and power system coupled with cascaded latent heat thermal energy storage based on supply-demand energy-exergy matching, Energy Convers. Manag. 268 (2022), 116040, https://doi.org/10.1016/j.enconman.2022.116040.

[45] F. Pilati, G. Lelli, A. Regattieri, M. Gamberi, Intelligent management of hybrid energy systems for techno-economic performances maximisation, Energy Convers. Manag. 224 (2020), 113329, https://doi.org/10.1016/j.enconman.2020.113329.

[46] K. Deb, A. Pratap, S. Agarwal, T. Meyarivan, A fast and elitist multiobjective genetic algorithm: NSGA-II, IEEE Trans. Evol. Comput. 6 (2002) 182–197, https://doi.org/10.1109/4235.996017.

[47] K. Deb, H. Jain, An evolutionary many-objective optimization algorithm using reference-point-based nondominated sorting approach, part I: solving problems with box constraints, IEEE Trans. Evol. Comput. 18 (2014) 577–601, https://doi.org/10.1109/TEVC.2013.2281535.

[48] I. Das, J.E. Dennis, Normal-boundary intersection: a new method for generating the pareto surface in nonlinear multicriteria optimization problems, SIAM J. Optim. 8 (1998) 631–657, https://doi.org/10.1137/S1052623496307510.

[49] F. Hameed, M. al Hosani, H.H. Zeineldin, A modified backward/forward sweep load flow method for islanded radial microgrids, IEEE Trans Smart Grid. 10 (2019) 910–918, https://doi.org/10.1109/TSG.2017.2754551.

[50] G.W. Chang, S.Y. Chu, H.L. Wang, An improved backward/forward sweep load flow algorithm for radial distribution systems, IEEE Trans. Power Syst. 22 (2007) 882–884, https://doi.org/10.1109/TPWRS.2007.894848.

[51] R.A. Krohling, A.G.C. Pacheco, A-TOPSIS - an approach based on TOPSIS for ranking evolutionary algorithms, Procedia Comput Sci. 55 (2015) 308–317, https://doi.org/10.1016/j.procs.2015.07.054.

[52] M. Potkány, M. Hlatká, M. Debnár, J. Hanzl, Comparison of the lifecycle cost structure of electric and diesel buses, Nase More. 65 (2018) 270–275, https://doi.org/10.17818/NM/2018/4SI.20.
[53] Fuel price calculator: How much do you pay? - BBC News, (n.d.). https://www.bbc.co.uk/news/business-21238363 (accessed February 11, 2023).
[54] Kg CO2 per litre of diesel vehicles | Comcar, (n.d.). https://comcar.co.uk/emissions/co2litre/?fueltype=diesel (accessed February 11, 2023).
[55] ESO Data Portal: National Carbon Intensity Forecast - Dataset| National Grid Electricity System Operator, (n.d.). https://data.nationalgrideso.com/carbon-intensity1/national-carbon-intensity-forecast (accessed February 11, 2023).
[56] CO_2 emission performance standards for cars and vans, (n.d.). https://climate.ec.europa.eu/eu-action/transport-emissions/road-transport-reducing-co2-emissions-vehicles/co2-emission-performance-standards-cars-and-vans_en (accessed February 11, 2023).